

Soft Matter

Accepted Manuscript



This is an *Accepted Manuscript*, which has been through the Royal Society of Chemistry peer review process and has been accepted for publication.

Accepted Manuscripts are published online shortly after acceptance, before technical editing, formatting and proof reading. Using this free service, authors can make their results available to the community, in citable form, before we publish the edited article. We will replace this *Accepted Manuscript* with the edited and formatted *Advance Article* as soon as it is available.

You can find more information about *Accepted Manuscripts* in the [Information for Authors](#).

Please note that technical editing may introduce minor changes to the text and/or graphics, which may alter content. The journal's standard [Terms & Conditions](#) and the [Ethical guidelines](#) still apply. In no event shall the Royal Society of Chemistry be held responsible for any errors or omissions in this *Accepted Manuscript* or any consequences arising from the use of any information it contains.

**Milestone in the N_{TB} Phase Investigation and Beyond: Direct Insight
into Molecular Self-Assembly**

Trpimir Ivšić^a, Marijana Vinković^b, Ute Baumeister^c, Ana Mikleušević^a and Andreja
Lesac^{a*}

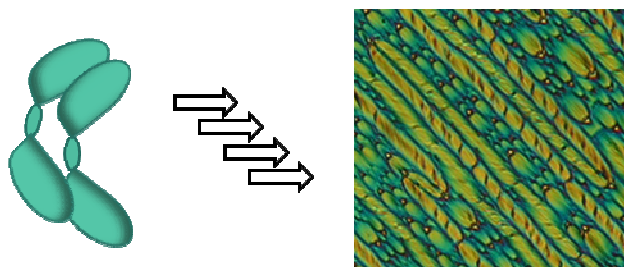
^a Division of Organic Chemistry and Biochemistry, Ruđer Bošković Institute, Bijenička cesta 54,
10000 Zagreb, Croatia,

^b NMR Center, Ruđer Bošković Institute, Bijenička cesta 54, 10000 Zagreb, Croatia,

^c Institute of Chemistry, Physical Chemistry, Martin Luther University Halle-Wittenberg, von-
Danckelmann-Platz 4, 06120 Halle, Germany.

Table of contents entry

The synergy of experimental, computational and NMR studies suggests a *syn*-parallel helical molecular organization within the N_{TB} phase.



Abstract

Although liquid-crystalline materials are most widely exploited for flat-panel, their ability to self-organize into periodically ordered nanostructures gives rise to a broad variety of additional applications. The recently discovered low-temperature nematic phase (N_{TB}) with unusual characteristics generated considerable attention within the scientific community: despite the fact that the molecules from which the phase is composed are not chiral, the helicoidal structure of the phase is strongly implicated. Here we report on combined experimental, computational, and spectroscopic studies of the structural aspects influencing formation of the N_{TB} phase as well as on the molecular organization within the phase. In an extensive DFT study, the structure-property prerequisite was traced to a "bent-propeller" shape of the molecule. We also demonstrate the first utilization of liquid state NMR for direct analysis of intermolecular interactions within thermotropic liquid-crystalline phases, providing the new insight into molecular packing that can lead toward design of novel chiral functional materials. The synergy of experimental, computational and NMR studies suggests a *syn*-parallel helical molecular organization within the N_{TB} phase.

INTRODUCTION

The nematic liquid-crystalline phase, the best known for its exceptionally successful implementation in flat panel displays, is characterized by such organization in which molecules keep their long axes locally parallel on the average, but the centers of mass have no positional order. This simple molecular arrangement may be swayed by the introduction of chirality, which leads to the cholesteric phase (chiral nematic, N^*) or to the blue phase (BP). In 1973 Meyer¹ suggested a theoretical possibility for the existence of a twist-bend nematic (N_{TB}) phase, in which the director of the molecules would precess on a cone forming an oblique helicoidal structure. More recently Dozov² and Memmer³ demonstrated that the formation of the N_{TB} phase does not require molecular chirality, instead it can be facilitated by the shape of bent molecules.

And yet, it was only a few years ago, that the unknown nematic phase (N_x) was also experimentally observed, whose unusual characteristic implicated the N_{TB} structure.⁴⁻¹⁰ A puzzling combination of smectic textural features but absence of the smectic-like lamellar X-ray diffraction peaks boosted the interest for this new nematic phase. A series of studies^{6,9,11-15} focused on investigation of the low-temperature nematic phase formed by 1,7-di-(1"-cyanobiphenyl-4-yl)heptane (**CB7CB**) reported an evidence for the chiral molecular organization, which is consistent with an oblique helicoidal structure. These observations include: focal conic, polygonal and rope-like textures displayed by polarizing optical microscopy,⁶ helix periodicity observed directly by freeze-fracture transmission electron microscopy (FFTEM),^{9,11} flexoelectrically driven electroclinic effect showing extremely short pitch (<10 nm) and ultrafast response times,¹² and discrimination of the prochiral protons in deuterium NMR experiments.¹³⁻¹⁵ However, several aspects of the phase are still the subjects of the debate: high viscosity, lack of temperature dependence of the TB helix pitch,¹¹ presence of various periodicity ranging from 7.7 to 3.4 nm,⁹ suppression of induced helicity with the addition of chiral

dopants, no electrooptic response in the N_{TB} phase of **CB11CB**¹⁶ and locked helical structures of a particular pitch.¹⁷

For the majority of the odd-membered dimers displaying two nematic phases, the common structural feature is the methylene link between the spacer and the rigid mesogenic groups.^{5,9} However, the presence of the N_x phase has also been reported for some odd-membered dimers with an imino linkage.^{4,8} Due to the limited number of structurally variant compounds exhibiting the low-temperature nematic phase, there is still little known about the structural and electronic aspects influencing its formation.

Herein we report the observation of the N_{TB} phase for some new odd-membered imino-linked cyanobiphenyls that enable a comparative study with methylene and ether linked cyanobiphenyls on impact of the linkage group. In order to unravel the role of structural and electronic factors on the formation of the N_{TB} phase, we have performed a detailed conformational analysis of the methylene, ether and imino linked cyanobiphenyls, as well as the less polar **BB_7-4**. Most importantly, we will show that common liquid state NMR can be applied for direct elucidation of intra- and intermolecular interactions within both nematic phases – the first of a kind for studying liquid-crystalline phases. Finally, based on the combined experimental, computational, and spectroscopic studies, we propose a molecular organization within the N_{TB} phase.

RESULTS AND DISCUSSION

Mesomorphic properties.

The studied materials and their thermal behavior are shown in Figure 1.

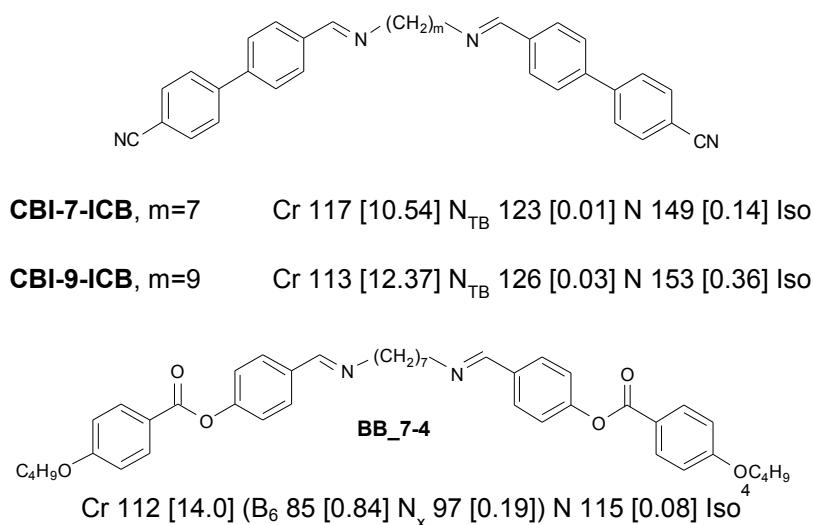


Figure 1. Molecular structures and thermal behavior of the studied materials. Monotropic transitions are given in parenthesis, transition temperatures in °C, and the dimensionless value of $\Delta S/R$ in brackets. Cr, crystalline phase; N_{TB}, low-temperature nematic phase; N, nematic phase; Iso, isotropic liquid.

The mesomorphic behavior of the dimers **CBI-7-ICB** and **CBI-9-ICB** was determined using polarizing optical microscopy (POM), differential scanning calorimetry (DSC) and X-ray diffraction (XRD). Both dimers display similar mesomorphic properties. Upon heating they show three phase transitions: melting, followed by the N_{TB}-N transition and isotropization. A nematic phase was identified by the typical marbled texture. The lower temperature mesophase was assigned as N_{TB} phase by direct analogy with the behavior found in **CB7CB**⁶, **CB11CB**¹⁶ and benzyloxybenzilidene⁴

dimers. In the cooling cycle the N_{TB} phase exhibits a particular textural sequence. The $N-N_{TB}$ transition was accompanied by a change in texture from the marble to a broken fan-like arrangement. Further cooling resulted in the formation of an elliptical polygonal domain texture from which a characteristic striped structure developed. Two distinct types of rope-like stripes are identified exhibiting a color exchange upon rotating the polarizer by $\pm 20^\circ$ (Figures 2a, b), thus suggesting enantiomorphism. Contact preparations showed complete miscibility of the N_x phase exhibited by the benzoyloxybenzylidene dimer⁴ and the low temperature mesophase of **CBI-7-ICB** and **CBI-9-ICB**, confirming that all three imino-linked dimers form the same phase. The results of the XRD measurements on **CBI-7-ICB** and **CBI-9-ICB** in the nematic phases on cooling from the isotropic liquid also closely resemble those for **CB7CB**.⁶ Samples aligned in a magnetic field show two kinds of diffuse halos in the wide angle and in the small angle regions, respectively, in both nematic phases. The d values for the maxima of the outer scattering at about 4.4 Å correspond to the lateral distances of the molecules, those of the inner scattering at about 14 Å for **CBI-7-ICB** and at about 15 Å for **CBI-9-ICB** are less than half the molecular lengths. The main effect at the phase transition $N - N_{TB}$ found by XRD is a change of the alignment and a loss of orientation (Figures 2c, d and Figure S1), but also the behavior of the d values for the maxima of the inner scattering with temperature changes at the phase transition as already found for $N - N_{TB}$ transitions.⁹ The d values grow with decreasing temperature in the nematic phase, they decrease within the N_{TB} phase from 14.0 (22 °C) to 13.5 Å (116 °C) for **CBI-7-ICB** and from 15.4 (126 °C) to 14.7 Å (116 °C) for **CBI-9-ICB** (Figure 2e, Figure S1 and Table S1).

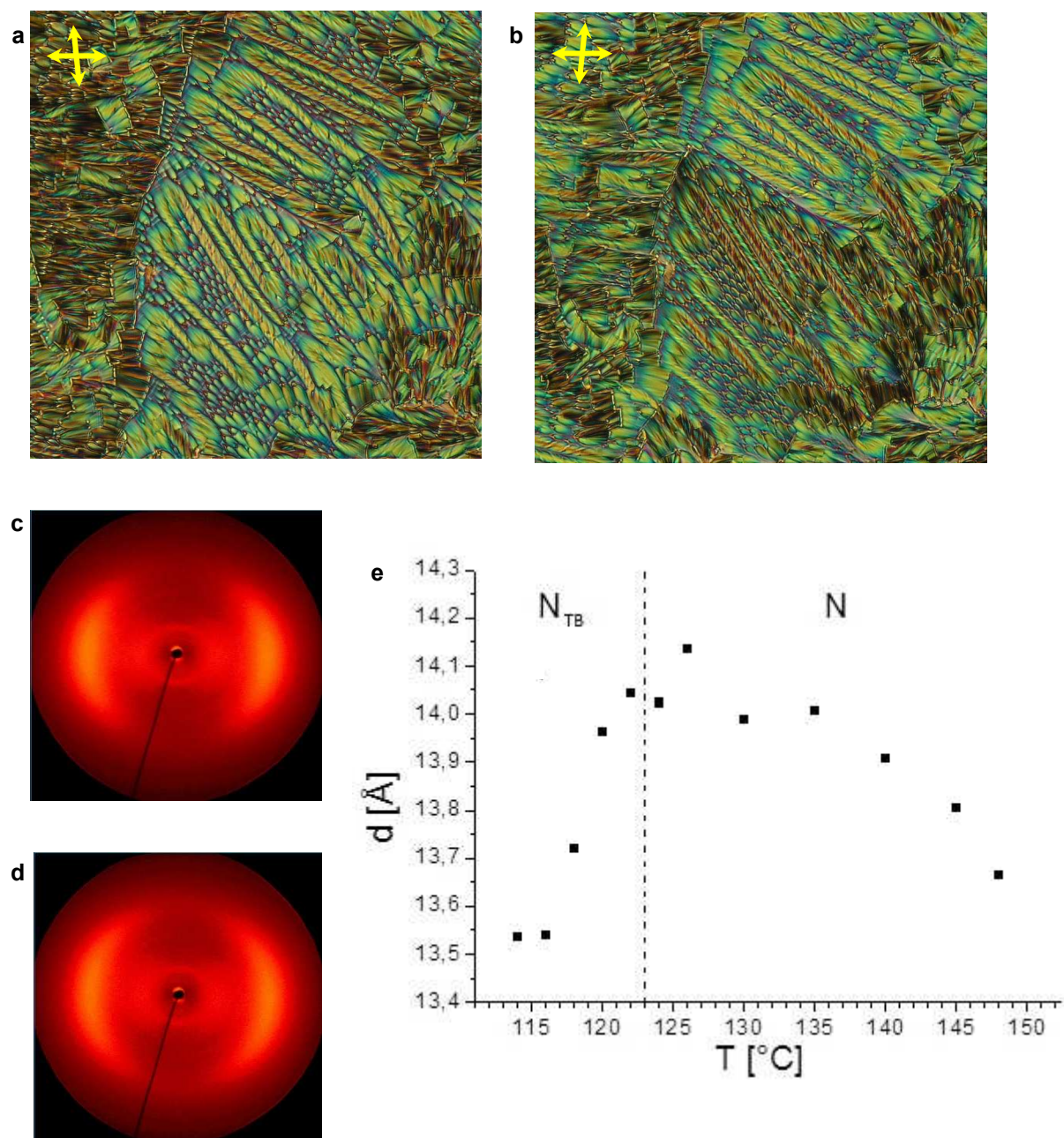


Figure 2. Rope-like texture of the N_{TB} phase of CBI-7-ICB obtained on cooling at 118°C , in thin cells without surface treatment with the polarizer and analyzer uncrossed: (a) by -20° , (b) by $+20^\circ$, and XRD patterns of both nematic phases on cooling aligned in the magnetic field: (c) 2D wide angle XRD pattern in the N phase at 135°C , (d) 2D wide angle XRD pattern in the N_{TB} phase at 118°C (the comparatively broad diffuse inner scattering on the equator of the patterns originates from the “Bremsberg” radiation of the only Ni-filtered Cu radiation and corresponds to the strong outer

diffuse scattering), (e) d value of the intensity maximum of the inner halo depending on the temperature.

It is well known that the transitional properties of liquid-crystalline dimers strongly depend on the molecular shape, which originates from both, the parity of atoms in the spacer and the type of functional group linking the spacer to the mesogenic units.¹⁹ The latter determines an angle between the *para*-axis of the mesogenic unit and the first bond in the spacer, which then results in biaxiality of the molecule.²⁰ A comparative study of odd-membered methylene (CBmCB) and ether (CBOmOCB) linked cyanobiphenyl dimers demonstrates that the methylene group provides a smaller link angle (113°) than the ether (126°), thus the slightly greater molecular biaxiality of the former. As a result, the clearing entropy is smaller for methylene linked dimers than for those with an ether link.^{21,22} Another significant difference between this two kinds of dimers is that the ether-linked dimers form only a single nematic phase,²³ while those with methylene links exhibit also a second liquid-crystalline phase.⁶ Recently, this additional mesophase was described as a twist-bend nematic phase and has been attributed to the more pronounced molecular bending.⁵⁻⁷

The both newly described imino-linked cyanobiphenyls, **CBI-7-ICB** and **CBI-9-ICB**, display two nematic phases and their thermal properties more resemble those of the methylene-linked derivatives than those with the ether links. For example, the observed entropy changes ($\Delta S/R$) associated with the N-I as well as the N-N_{TB} transitions for **CBI-7-ICB** and **CBI-9-ICB** are comparable in magnitude with the same transitions of dimers having methylene linkage.⁵⁻⁷ Similar behavior is noticed for benzyloxybenzilidene⁴ and salicyl⁸ based dimers, both possessing the imino links.

The Molecular Geometry - DFT Calculations.

To evaluate the influence of the linkage group and to gain a better understanding of the forces governing the molecular packing, an extensive computational study with focus on the linkage group was performed using the Gaussian software package.²⁴ The input geometries were based on the initial optimization of the mesogen⁸ connected with the spacer in the already established all-trans configuration of the carbon atoms.¹⁴

For the analysis of each dihedral rotation, series of single point constrained geometry optimizations were performed on B3LYP/6-31G level. The rotational barriers were then calculated as energy differences between the two limit geometries. The lowest energy structures were reoptimized using the B3LYP, wB97xD and M06-D3²⁵ functionals and 6-31G(d,p) basis set with tight convergence criteria.

From the chemistry of biphenyl, its derivatives are known to possess axial chirality, due to the rotation around the bond connecting two phenyl cores. Indeed, the fully optimized structure of **CBI-7-ICB** revealed that the two phenyl cores are mutually rotated by 36° around the biphenyl bond, and that the smallest energy barrier for rotation was ~1.7 kcal mol⁻¹. However, since the biphenyl rotation is also present in ether derivatives for which the N_{TB} phase is not observed, it can safely be excluded as a major factor determining the formation of the phase.

Further, it was suggested that the curvature of the molecule is responsible for the formation of the N_{TB} phase.²⁰⁻²² Upon optimization, the variation of the link angle between the linking groups was rather small. Comparing all three cyanobiphenyl derivatives, the methylene and imine derivatives were found slightly more bent than the ether derivative. The analogous C₁-C₂-N₃, C₁-C₂-C₃ and C₁-O₂-C₃ angles were 111°, 112° and 118°, respectively, the latter two being close to the reported ones²⁰⁻²². However, such proximity of the values and the existence of the N_{TB} phase in the rigid bent-core piperazyl derivate **UD68**,¹⁰ (the core bend angle is estimated to 120°), imply that the

Figure 3. Definition of dihedral rotation (τ) and comparison of imine- (\blacktriangledown), methylene- (\bullet) and ether-linked (\blacksquare) cyanobiphenyls

In the low energy state of the imine derivate, the dihedral angle between Π_M and Π_S may adopt two distinct values, approximately of the same magnitude ($\sim\pm 60^\circ$), but opposite sign. In analogy to the nomenclature used for the description of axial chirality, the right handed rotamer may be denoted with (*R*), and the left handed rotamer with (*S*). Since they have equal energy, their distribution in bulk sample should be equal. Thus, for the dimer molecule, two distinct enantiomeric conformers may be identified as (*R*)-(*R*) and (*S*)-(*S*), along with the third, *meso*-conformation (*R*)-(*S*). Analogous dihedral rotation for the **BB_7-4** derivate shows the same behavior, as a general property of the imino linked dimers. This feature of the imino linkage group is due to the asymmetry of the nitrogen atom possessing a single lone pair, causing the preferential alignment of the plane of the C=N double bond towards one of the two enantiotopic protons of the neighboring -CH₂- in the spacer.

Upon optimization, ether and methylene derivatives show a major difference regarding the angle between the planes Π_M and Π_S . A dihedral angle of $\tau = 0^\circ$ was obtained for the ether derivate, while $\tau = 93^\circ$ was found for the methylene derivate. Consequently, the geometric shape of the former is flat, while that of the latter is spacious, suggesting a different behavior when packing within the phase. In addition, in the ether a higher energy barrier for dihedral rotation was found (3.50 kcal mol⁻¹ compared to 0.89 kcal mol⁻¹) at M06-D3/6-31G(d,p) level. This indicates a more rigid conformation of the ether derivate. For methylene, a partial dihedral rotation may be allowed that would break the symmetry of the molecular conformation and cause the two hydrogens to be in a different chemical surrounding. Solid state NMR study of deuterated **CB7CB** reported that these two enantiotopic

hydrogens of the methylene linkage group have lost their equivalence just upon the formation of the N_{TB} phase.⁶

The direction of the dipole momentum in all the studied dimers is perpendicular to the main molecular axis (besides the *meso*-conformation of imine), due to the symmetrical arrangement of the polar mesogen units around the spacer. The methylene derivate is substantially more polar than ether (7.2 Debye compared to 2.3 Debye), since it lacks the polar C=O group producing charge in the direction opposite to the cyano group. Concerning the imine derivatives, **CBI-7-ICB** is more polar than **BB_7-4**, (6.0 and -4.8 Debye respectively). Note also that the dipoles have opposite signs. Both imine derivatives show the N_{TB} phase, as does the salicyl based imino-linked dimer **NS_7-8**⁸ whose polarity is rather low (0.1 Debye). Altogether we found no evidence that the magnitude of the dipole moment is responsible for the formation of the phase, as is also suggested by Mandle et al.²⁶ On the contrary, it is more likely that the geometry of the molecule is the decisive factor. Until now it was accepted that molecules forming N_{TB} phase need to be bent or "banana-shaped".^{2,3,9} On the basis of our results, a more precise analogy may be "twisted-banana" or even "bent-propeller", accounting for the large dihedral angle between the plane of mesogen and the plane common to carbon atoms in the spacer.

Intermolecular Interactions - ¹H NMR study.

In addition to the molecular shape, a macroscopic structure is greatly determined by the molecular interactions. In the nematic phases, interactions between molecules should be statistically random, since only an orientational ordering is present. In contrast, in the low temperature nematic phase presence of the focal conic texture and absence of layer reflections imply a long range periodic ordering that may be due to a helical macrostructure.

Although XRD is a powerful tool for the determination of the molecular arrangement within liquid-crystalline phases, its application for the study of the N_{TB} phase is limited. Therefore, it became of interest to find another method that could be applied for analyzing the molecular packing within the mesophase.

NMR spectroscopy is used to determine the structures, dissect molecular interactions, and investigate the dynamics of liquid-crystalline phases.²⁷ Various solid state NMR techniques have been intensively used in liquid crystal research^{6,13,28,29} yielding precise information on molecular structure and conformation. However, the knowledge of intermolecular interactions in the phase gained by liquid state NMR methods would provide much deeper insight into the packing mode. Numbers of routine NMR methods are available, that are daily used for the characterization of matter in solution. Of particular interest are methods such as NOESY which is typically used for describing interactions of atoms through space at the distance of $\leq 5 \text{ \AA}$, whether these interactions are intermolecular or intramolecular. To the best of our knowledge none of them has been applied on the bulk sample in the N_{TB} phase or in liquid-crystalline phases in general.

Comparison of ^1H NMR spectra of **CBI-7-ICB** and **BB_7-4** recorded in CDCl_3 solution (Figure S2) shows that the latter is more suitable for a study of NOE interactions than the cyanobiphenyl series. The signals of aromatic protons in cyanobiphenyls overlap to some extent, while in **BB_7-4** they are conveniently resolved. Moreover, the terminal alkyl chain may provide more data on the head-to-tail interactions between the molecules than the protonless cyano group.

Figure 4. (a) ^1H NMR spectra of **BB_7-4** in $\text{DMSO-}d_6$ solution. (b) ^1H NMR spectra of the neat **BB_7-4** recorded in the cooling cycle at 110 °C, 90 °C and 80 °C in comparison with the DSC thermogram. (c) NOESY spectra of the neat **BB_7-4** recorded at 90 °C and 110 °C. (d) Sketch of the most pronounced intermolecular NOESY interactions at 90°C.

For the neat **BB_7-4**, our study revealed that liquid state NMR may be recorded in the temperature range of both nematic phases. All the proton signals were shielded and moved to higher magnetic field by 0.68 to 1.09 ppm in comparison to solution due to molecular crowding (Figure 4a, b). The signals are significantly broadened and coupling constants are not visible. However, starting from the I-N transition at 115°C and cooling down at a very slow cooling rate (0.5 °C/min), the ^1H NMR signals started to diminish at ~84 °C, although they were visible down to ~80 °C, which corresponds to the temperature of crystallization. The proton signals were assigned as shown in Figure 4b using ^1H and $^1\text{H-}^1\text{H}$ COSY spectra of the neat compound in the N_{TB} phase at 90 °C (Table S2 and Figure S3). The NOESY spectra were recorded at 110 °C, 100 °C (nematic phase) and 90 °C (N_{TB} phase), respectively. All the visible NOE interactions at 110 °C (Figure 4c) are between protons that are no more than ~4.7 Å apart in the molecular structure of **BB_7-4** and thus most likely of the intramolecular kind. At 90 °C new interactions appear (Figure 4c), and the distance between the protons assigned to these interactions (not present at 110 °C) surpasses the NOE measurement threshold. For example, the interactions of H15 with H11; H6 with H1 and H2; H7 with H2 and H3 (Figure 4c, d) become clearly visible at 90 °C, all of which are more than 5 Å apart in the individual molecular structure. These can be attributed only to intermolecular interactions between the two neighboring molecules in a repeating motive out of which the molecular packing in N_{TB} phase is predominantly formed. In control experiment, NOESY spectra have been taken in $\text{DMSO-}d_6$ solution at 50 °C and in CDCl_3 solution at -40 °C (Figure S4), and the intramolecular interactions between hydrogen atoms only up to 2.5 Å apart were observed. Altogether, the former experiments

present an unambiguous proof for the existence different molecular organization at 110 °C in the nematic and at 90 °C in the N_{TB} phase, and are also the first liquid state NMR spectroscopy of that kind in liquid crystals.

In addition we have noticed that the supramolecular organization begins to form already in the nematic, a few degrees above the $N-N_{TB}$ transition, as observed in NOESY spectra recorded at 100 °C, (Figure S5). The intermolecular interactions found in the N_{TB} phase are also present here, although, they are much smaller in magnitude on 100 °C than on 90 °C. This confirms the incipience of a dynamic formation of small clusters prior to the $N-N_{TB}$ transition, which can also cause the diffuse X-ray diffraction in the small angle region within the nematic phase.

Concerning the exact nature of intermolecular packing, the currently proposed model for the N_{TB} phase is based on an *anti*-parallel orientation of the mesogens where the molecules form a helical structure *via* intercalation (Figure 5a).^{10,12} While this would require protons of the alkyl chain (H1-H4) to be in the vicinity of protons next to the linkage group, H14 and H15, and of the neighboring aromatic H11 and H12, strong interactions in the NOESY spectra would be expected at least between some of them. To our surprise, those interactions are not visible in the spectra of the N_{TB} phase (90 °C). However, all the visible NOE interactions in the N_{TB} phase point to a *syn*-parallel orientation of the mesogens (Figure 5b) featuring parallel displacement of the molecules to stabilize the π - π interactions. Preliminary DFT calculations for the two types of packing also suggest that the *syn*-arrangement is by 22.5 kcal mol⁻¹ energetically more favorable than the *anti*-arrangement on M06-D3/6-31G(d,p), although the complete conformational landscape was not explored due to the size of the system.

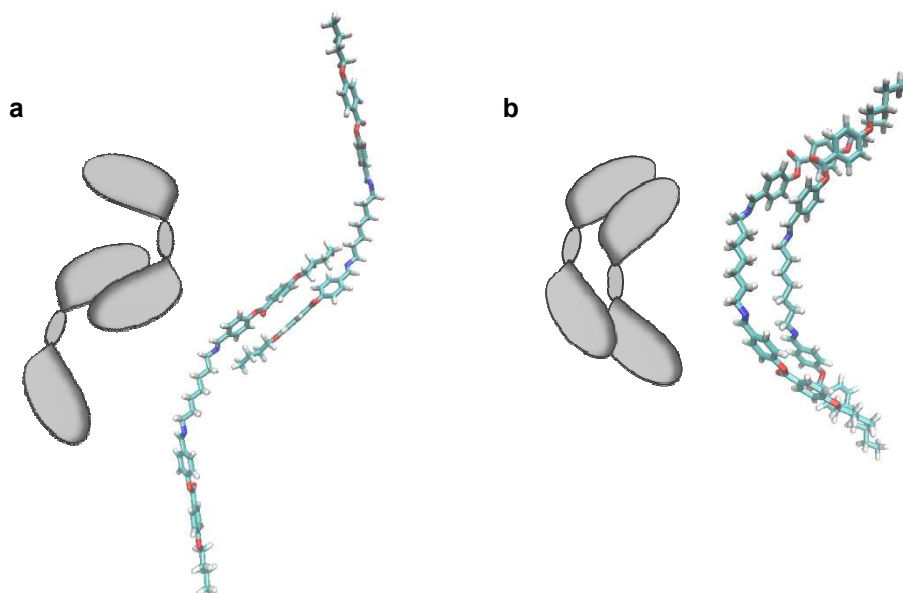


Figure 5. Models and preliminary structures after optimization on M06-D3/6-31G(d,p): (a) *anti*-parallel arrangement of mesogens, (b) *syn*-parallel arrangement of mesogens.

Thus the *syn*-parallel packing motive is very much in agreement with both, the DFT calculations (Figure 5b) and the interactions experimentally found in NOESY (Figure 4d). Upon optimization, two molecules in "bent-propeller" conformation are displaced in parallel direction in order to stabilize the π - π interactions. Such arrangement puts the key atoms from the two molecules to be within the NOE measurement threshold, which would produce the observed intermolecular interactions. Notably, due to the stabilization, the molecules in *syn*-parallel packing motive are also slightly rotated in respect to each other. Thus, the multiple repetition of the *syn*-parallel displacement packing motive determined by NOESY would produce a helical formation with the director of the molecules precessing around the helical axis (Figure 6). In contrast to the proposed intercalated organization, in our model of the N_{TB} phase the molecules are through self-assembly organized in stepwise manner. Direction of the formed helix is determined by the exact conformation of molecules in unit packing motive, so in principle both P and M enantiomorphs may

be expected to coexist in bulk sample. The organization of helices towards the larger chiral domains remains to be concluded.

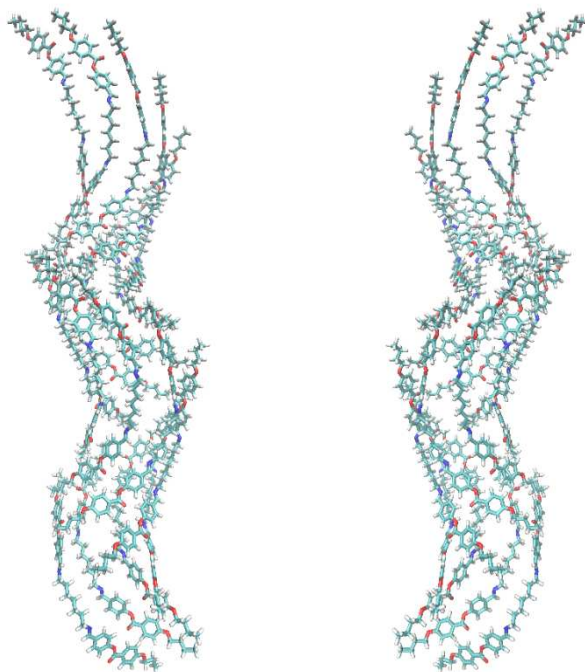


Figure 6. Model for helical self-assembly obtained by multiple repetition of *syn*-parallel packing motive and its mirror image

EXPERIMENTAL SECTION

General Information.

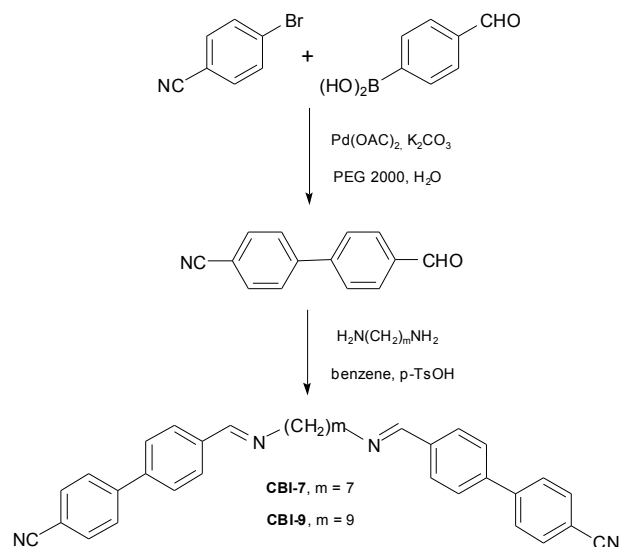
All the solvents were either *puriss p.a.* quality or distilled over appropriate drying reagents. All the other reagents were used as purchased from Aldrich. NMR spectra were recorded on Bruker AV-600 instrument in DMSO- d_6 with SiMe $_4$ as internal standard unless stated otherwise. Phase transition temperatures and textures were determined using an Olympus BX51 polarizing microscope equipped with a Linkam TH600 hot stage and PR600 temperature controller. Enthalpies

of transition were determined from thermograms recorded on Perkin-Elmer Diamond DSC, operated at scanning rates of $5\text{ }^{\circ}\text{C min}^{-1}$. To perform X-ray diffraction measurements samples of **CBI-7-ICB** and **CBI-9-ICB** were kept in glass capillaries (\varnothing 1 mm) in a temperature controlled heating stage and partially aligned in a magnetic field on cooling (1 K/min) from the isotropic liquid. 2D patterns were recorded by an area detector VÅNTEC500 (Bruker AXS) using Ni-filtered $\text{CuK}\alpha$ radiation. The one- and two dimensional homo- and heteronuclear ^1H and ^{13}C NMR spectra were recorded with a Bruker AV-600 spectrometer, operating at 600.133 MHz for the ^1H nucleus and 150.917 MHz for the ^{13}C nucleus. The following measurement techniques were used: standard ^1H , ^{13}C gated proton decoupling, APT, COSY, NOESY, HMQC and HMBC. To record the NMR spectra in the liquid crystalline phase the glass capillary (\varnothing 1 mm) filled with solid compound was immersed into standard 5 mm NMR tube filled with DMSO-d_6 . Sample was melted and put in warmed up spectrometer on high temperature (115 $^{\circ}\text{C}$). The temperature is regulated by a Bruker B-VT 3000 temperature unit. Slowly cooling down the instrument (0.5 $^{\circ}\text{C}/\text{min}$), ^1H spectra were taken in series on various temperatures. Each spectrum was taken after preheating to 110 $^{\circ}\text{C}$ and slow cooling down to 100 $^{\circ}\text{C}$ or 90 $^{\circ}\text{C}$. Chemical shifts are reported in ppm, downfield of tetramethylsilane. FID resolution in ^1H NMR and ^{13}C NMR spectra was 0.29 Hz and 0.54 Hz per point, respectively. The NOESY spectra were measured in phase-sensitive mode, with mixing time of 0.50 s and 16 or 64 scans per each increment. The spectral width was 6127.45 Hz, 2048 points in F2 dimension and 512 increments in F1 dimension, subsequently zero-filled to 1024 points. The resulting FID resolution was 2.99 Hz/point and 11.96 Hz/point in F2 and F1 dimensions, respectively.

Synthesis.

The novel imino-linked cyanobiphenyl dimers **CBI-7-ICB** and **CBI-9-ICB** were prepared from 4-bromo-benzonitrile and 4-formylphenylboronic acid employing Suzuki coupling¹⁸ followed by condensation with appropriate α,ω -diamino alkane (Scheme 1). $\text{N,N}'\text{-bis}[4'-(4''-$

butyloxybenzoyloxy)benzylidene]-heptane-1,7-diamine (**BB_7-4**) was prepared as described previously and its physical properties are consistent with the published data.⁴



Scheme 1. Synthesis of imino-linked cyanobiphenyl dimers **CBI-7-ICB** and **CBI-9-ICB**.

*4-Formyl-biphenyl-4'-carbonitrile*¹⁸ A mixture of Na_2CO_3 (1.06 g, 10 mmol), Pd(OAc)_2 (56 mg, 5 mol %), PEG 2000 (17.5 g) and water (15 mL) was heated to 50 °C under inert atmosphere with stirring. Afterwards, 4-bromo-benzonitrile (0.91 g, 5 mmol) and 4-formylphenylboronic acid (1.12 g, 7.5 mmol) were added to the solution, and the reaction was carried out at 50 °C under inert atmosphere. After 45 min. the reaction mixture was cooled to room temperature, diluted with water (100 mL), and extracted with diethyl ether (3 x 50 mL). The combined organic extracts were washed with brine (50 mL), dried over anhydrous Na_2SO_4 and concentrated in vacuum. The crude product was purified by column chromatography on silica gel using CH_2Cl_2 as eluent affording product (0.88 g, 85 %) as white solid. mp. 59-160 °C; $^1\text{H-NMR}$ (CDCl_3) δ /ppm: 7.72-7.80 (m, 6H), 8.00 (d,

$J=8.4$ Hz, 2H), 10.09 (s, 1H); $^{13}\text{C-NMR}$ (CDCl_3) δ/ppm : 112.2, 118.5, 127.9, 128.0, 130.4, 132.8, 136.1, 144.1, 144.9, 191.6.

General procedure for the preparation of imines. A solution of the appropriate α,ω -diamine (1 mmol) in benzene (2 mL) was added dropwise to a hot solution of 4-formyl-biphenyl-4'-carbonitrile (2 mmol) in benzene (25 mL) and catalytic amount of *p*-toluenesulfonic acid. The reaction mixture was heated under reflux for 1 h under argon and then 15 mL of benzene was distilled off. The hot residue was filtered and mixed with *n*-hexane (25 mL). The pure crystalline product, which precipitated on cooling, was separated by filtration.

N,N'-bis(4,4'-cyanobiphenylmethylidene)-heptane-1,7-diamine, **CBI-7-ICB**. Yield, 60 %; PT ($^{\circ}\text{C}$): Cr 117 N_{TB} 123 N 149 Iso; $^1\text{H-NMR}$ (CDCl_3) δ/ppm : 1.41-1.47 (m, 6 H), 1.71-1.81 (m, 4H), 3.67 (t, $J=6.8$ Hz, 4H), 7.65 (d, $J=8.4$ Hz, 4H Ar), 7.71-7.78 (m, 8H Ar), 7.86 (d, $J=8.4$ Hz, 4H Ar), 8.34 (s, 2H); $^{13}\text{C-NMR}$ (CDCl_3) δ/ppm : 27.3, 29.2, 30.9, 61.9, 111.4, 118.8, 127.4, 127.7, 128.7, 132.6, 136.6, 141.0, 144.9, 159.9. Found: C, 82.50; H, 6.25; N, 11.13. Calc for $\text{C}_{35}\text{H}_{32}\text{N}_4$: C, 82.64; H, 6.34; N, 11.01.

N,N'-bis(4,4'-cyanobiphenylmethylidene)-nonane-1,9-diamine, **CBI-9-ICB**. Yield, 82 %; PT ($^{\circ}\text{C}$): Cr 113 N_{TB} 126 N 153 Iso; $^1\text{H-NMR}$ (CDCl_3) δ/ppm : 1.37-1.43 (m, 10 H), 1.69-1.79 (m, 4H), 3.66 (t, $J=6.8$ Hz, 4H), 7.66 (d, $J=8.3$ Hz, 4H Ar), 7.71-7.78 (m, 8H Ar), 7.86 (d, $J=8.3$ Hz, 4H Ar), 8.34 (s, 2H); $^{13}\text{C-NMR}$ (CDCl_3) δ/ppm : 27.3, 29.4, 29.5, 30.9, 61.9, 111.3, 118.8, 127.4, 127.7, 132.6, 136.6, 140.9, 144.9, 159.8. Found: C, 82.68; H, 6.73; N, 10.57. Calc for $\text{C}_{37}\text{H}_{36}\text{N}_4$: C, 82.80; H, 6.76; N, 10.44.

CONCLUSION

In summary, some new cyanobiphenyl dimers with an imino linkage group are reported to show the N_{TB} phase. A comparative computational study of the methylene, ether and imino linked cyanobiphenyls, as well as the less polar imino linked benzyloxybenzylidene **BB_7-4** showed that the geometry of the molecule is the predominating factor in the formation of the N_{TB} phase. In addition to the already known requirement for the curvature of the molecule, the twist caused by the dihedral angles between the plane of the spacer and the planes of the mesogens was identified as an important structural difference between the compounds with and without the N_{TB} phase. We have also demonstrated the first utilization of liquid state NMR for direct analysis of intermolecular interactions within liquid-crystalline phases. Comparison of the NOESY spectra of the neat sample in the N and N_{TB} phases revealed a *syn*-parallel orientation of the mesogens within the N_{TB} phase suggesting a *syn*-parallel helical molecular organization. Overall, the employment of liquid state NMR techniques provides direct insight into intermolecular interactions, which in combination with other experimental, computational, and spectroscopic methods significantly contributes to the elucidation of the molecular organization within the controversially discussed N_{TB} phase.

Electronic Supplementary Information (ESI) available:

ACKNOWLEDGEMENTS

The authors thank the Ministry of Science, Education and Sports of the Republic of Croatia for financial support (grant nos 098-0982933-2908, 098-0982904-2910, 098-0982929-2917). We are also grateful to Dr. Nađa Došlić (Theoretical Chemistry Group, Ruđer Bošković Institute, Zagreb)

for helpful discussions and suggestions concerning the electronic structure calculations and to Prof. Janez Plavec (Slovenian NMR Centre, National Institute of Chemistry, Ljubljana, Slovenia) for helpful discussions regarding NMR spectra.

REFERENCES

- 1 R. Balian and G. Weill, *Molecular Fluids Les Houches Lectures 1973*, Routledge, London u.a., 1976.
- 2 I. Dozov, *EPL Europhys. Lett.*, 2001, **56**, 247–253.
- 3 R. Memmer, *Liq. Cryst.*, 2002, **29**, 483–496.
- 4 M. Šepelj, A. Lesac, U. Baumeister, S. Diele, H. L. Nguyen and D. W. Bruce, *J. Mater. Chem.*, 2007, **17**, 1154–1165.
- 5 V. P. Panov, M. Nagaraj, J. K. Vij, Y. P. Panarin, A. Kohlmeier, M. G. Tamba, R. A. Lewis and G. H. Mehl, *Phys. Rev. Lett.*, 2010, **105**, 167801.
- 6 M. Cestari, S. Diez-Berart, D. A. Dunmur, A. Ferrarini, M. R. de la Fuente, D. J. B. Jackson, D. O. Lopez, G. R. Luckhurst, M. A. Perez-Jubindo, R. M. Richardson, J. Salud, B. A. Timimi and H. Zimmermann, *Phys. Rev. E*, 2011, **84**, 031704.
- 7 P. A. Henderson and C. T. Imrie, *Liq. Cryst.*, 2011, **38**, 1407–1414.
- 8 M. Šepelj, U. Baumeister, T. Ivšić and A. Lesac, *J. Phys. Chem. B*, 2013, **117**, 8918–8929.
- 9 V. Borshch, Y.-K. Kim, J. Xiang, M. Gao, A. Jákli, V. P. Panov, J. K. Vij, C. T. Imrie, M.-G. Tamba and G. H. Mehl, *Nat. Commun.*, 2013, **4**, 2635.
- 10 D. Chen, M. Nakata, R. Shao, M. R. Tuchband, M. Shuai, U. Baumeister, W. Weissflog, D. M. Walba, M. A. Glaser and J. E. MacLennan, *Phys. Rev. E*, 2014, **89**, 022506.
- 11 D. Chen, J. H. Porada, J. B. Hooper, A. Klittnick, Y. Shen, M. R. Tuchband, E. Korblova, , D. Bedrov, D. M. Walba and M. A. Glaser, *PNAS*, 2013, **110**, 15931–15936.
- 12 C. Meyer, G. R. Luckhurst and I. Dozov, *Phys. Rev. Lett.*, 2013, **111**, 067801.
- 13 L. Beguin, J. W. Emsley, M. Lelli, A. Lesage, G. R. Luckhurst, B. A. Timimi and H. Zimmermann, *J. Phys. Chem. B*, 2012, **116**, 7940–7951.

- 14 J. W. Emsley, M. Lelli, A. Lesage and G. R. Luckhurst, *J. Phys. Chem. B*, 2013, **117**, 6547–6557.
- 15 C. Greco, G. R. Luckhurst and A. Ferrarini, *Phys. Chem. Chem. Phys.*, 2013, **15**, 14961–14965.
- 16 R. J. Mandle, E. J. Davis, C. T. Archbold, S. J. Cowling and J. W. Goodby, *J. Mater. Chem. C*, 2014, **2**, 556–566.
- 17 A. Hoffmann, A. G. Vanakaras, A. Kohlmeier, G. H. Mehl and D. J. Photinos, 2014, *ArXiv Prepr. ArXiv14015445*.
- 18 L. Liu, Y. Zhang and Y. Wang, *J. Org. Chem.*, 2005, **70**, 6122–6125.
- 19 C. T. Imrie and P. A. Henderson, *Chem. Soc. Rev.*, 2007, **36**, 2096–2124.
- 20 A. Ferrarini, G. R. Luckhurst, P. L. Nordio and S. J. Roskilly, *Liq. Cryst.*, 1996, **21**, 373–382.
- 21 P. J. Barnes, A. G. Douglass, S. K. Heeks and G. R. Luckhurst, *Liq. Cryst.*, 1993, **13**, 603–613.
- 22 P. A. Henderson, J. M. Seddon and C. T. Imrie, *Liq. Cryst.*, 2005, **32**, 1499–1513.
- 23 J. W. Emsley, G. R. Luckhurst, G. N. Shilstone and I. Sage, *Mol. Cryst. Liq. Cryst.*, 1984, **102**, 223–233.
- 24 M. J. Frisch, G. W. Trucks, H. B. Schlegel, G. E. Scuseria, M. A. Robb, J. R. Cheeseman, G. Scalmani, V. Barone, B. Mennucci, G. A. Petersson, H. Nakatsuji, M. Caricato, X. Li, H. P. Hratchian, A. F. Izmaylov, J. Bloino, G. Zheng, J. L. Sonnenberg, M. Hada, M. Ehara, K. Toyota, R. Fukuda, J. Hasegawa, M. Ishida, T. Nakajima, Y. Honda, O. Kitao, H. Nakai, T. Vreven, J. A. Montgomery, Jr., J. E. Peralta, F. Ogliaro, M. Bearpark, J. J. Heyd, E. Brothers, K. N. Kudin, V. N. Staroverov, R. Kobayashi, J. Normand, K. Raghavachari, A. Rendell, J. C. Burant, S. S. Iyengar, J. Tomasi, M. Cossi, N. Rega, J. M. Millam, M. Klene, J. E. Knox, J. B. Cross, V. Bakken, C. Adamo, J. Jaramillo, R. Gomperts, R. E. Stratmann, O. Yazyev, A. J. Austin, R. Cammi, C. Pomelli, J. W. Ochterski, R. L. Martin, K. Morokuma, V. G. Zakrzewski, G. A. Voth, P. Salvador, J. J. Dannenberg, S. Dapprich, A. D. Daniels, Ö. Farkas, J. B. Foresman, J. V. Ortiz, J. Cioslowski, and D. J. Fox, GAUSSIAN 09 (Revision A.02), Gaussian Inc., Wallingford, CT, 2009.
- 25 S. Grimme, J. Antony, S. Ehrlich and H. Krieg, *J. Chem. Phys.*, 2010, **132**, 154104.
- 26 R. J. Mandle, E. J. Davis, S. A. Lobato, C.-C. A. Vol, S. J. Cowling and J. W. Goodby, *Phys. Chem. Chem. Phys.*, 2014, **16**, 6907–6915.
- 27 W. Feng, L. Pan and M. Zhang, *Sci. China Life Sci.*, 2011, **54**, 101–111.
- 28 R. Y. Dong, *Nuclear Magnetic Resonance Spectroscopy of Liquid Crystals*, World Scientific, Singapore, 2010.

29 A. Aluculesei, F. Vaca Chávez, C. Cruz, P. J. Sebastião, N. G. Nagaveni, V. Prasad and R. Y. Dong, *J. Phys. Chem. B*, 2012, **116**, 9556–9563.